Hydrodynamic equation of a spinor dipolar Bose-Einstein condensate

Kazue Kudo[1] and Yuki Kawaguchi[2]

[1]*Division of Advanced Sciences, Ochadai Academic Production, Ochanomizu University, 2-1-1 Ohtsuka, Bunkyo-ku, Tokyo 112-8610, Japan*
[2]*Department of Physics, University of Tokyo, 7-3-1 Hongo, Bunkyo-ku, Tokyo 113-0033, Japan*

We introduce equations of motion for spin dynamics in a ferromagnetic Bose-Einstein condensate with magnetic dipole-dipole interaction, written using a vector expressing the superfluid velocity and a complex scalar describing the magnetization. This simple hydrodynamical description extracts the dynamics of spin wave and affords a straightforward approach by which to investigate the spin dynamics of the condensate. To demonstrate the advantages of the description, we illustrate dynamical instability and magnetic fluctuation preference, which are expressed in analytical forms.

I. INTRODUCTION

One of the salient features of a gaseous Bose-Einstein condensate (BEC) is the internal spin degrees of freedom. In spinor BECs, namely, in BECs with internal degrees of freedom, spin and gauge degrees of freedom couple in various manners, leading to nontrivial properties of spin waves and topological excitations. For example, ferromagnetic BECs have continuous spin-gauge symmetry, thus the circulation of the superfluid velocity is not quantized [1–3], whereas spin-1 polar BECs and spin-2 cyclic BECs can host fractional vortices due to the discrete spin-gauge symmetry [4–7]. In recent experiments, *in situ* imaging of transverse magnetization has revealed the real-time dynamics of the spontaneous symmetry breaking, spin texture formation, and nucleation of spin vortices [8–10], opening up a new paradigm for studying the static and dynamic properties of spin textures.

On the other hand, BECs with magnetic dipole-dipole interaction (MDDI) have also attracted much attention both experimentally and theoretically in recent years. The long-range and anisotropic nature of the MDDI is predicted to yield exotic phenomena, such as new equilibrium shapes, roton-maxon spectra, supersolid states, and two-dimensional solitons [11]. In particular, when the BEC has spin degrees of freedom, the MDDI is predicted to develop spin textures, even when the MDDI is much weaker than the contact interaction [12–14]. This work is motivated by experiments done by the Berkeley group [9], where small magnetic domains were observed to develop from a helical spin structure in a spin-1 ^{87}Rb BEC. The method presented in this paper simplifies the spin dynamics in a complicated system of spinor dipolar BECs, although we have shown in our previous work that mean-field calculations do not reproduce the experimental results [15].

In this paper, we propose a hydrodynamic description of a ferromagnetic BEC with MDDI. The hydrodynamic equation of spinor BECs has been discussed for both ferro-magnetic phases [16–18] and nonmagnetized phases [18,19]. In Ref. [16], Takahashi *et al.* consider the strong MDDI limit by using the classical spin model, i.e., by neglecting the spin-gauge coupling. On the other hand, Lamacraft takes into account the spin-gauge coupling by introducing the so-called Mermin-Ho relation, and considers the weak MDDI [17]. In these papers, the authors use a unit vector to describe the local magnetization in the ferromagnetic phase. Here we use a single complex scalar variable instead of a unit vector to describe the local magnetization and treat both the spin-gauge coupling and MDDI. This simple description allows a straightforward approach to analyze the spin dynamics of the condensate. In order to demonstrate the advantages of our description, we analyze the dynamical instability and magnetization fluctuation preference of the BEC with MDDI.

The rest of the paper is organized as follows. In Sec. II, hydrodynamic equations described using the spin density vector are derived from the Gross-Pitaevskii (GP) equation. We then rewrite the equations by means of stereographic projection for some simple cases: quasi-two-dimensional (2D) systems under zero external field and under a strong magnetic field. For both zero-field and strong-field cases, the wave-vector dependence of the dynamical instability is obtained straightforwardly in an analytical form in Sec. III. In Sec. IV, we also illustrate the magnetic fluctuation preference for the unstable modes discussed in Sec. III. Conclusions are given in Sec. V.

II. HYDRODYNAMIC DESCRIPTION

A. Equations of motion of mass and spins

We consider a spin-F BEC under a uniform magnetic field B applied in the z direction. The GP equation for the spinor dipolar system is given by

$$i\hbar \frac{\partial}{\partial t}\Psi_m(\boldsymbol{r},t) = (H_0 + pm + qm^2)\Psi_m$$

$$+ \sum_{S=0,\text{even}}^{2F} \frac{4\pi\hbar^2}{M}a_S \sum_{M_S=-S}^{S} \sum_{n,m',n'=-F}^{F}$$

$$\times \langle mn|SM_S\rangle\langle SM_S|m'n'\rangle\Psi_n^*\Psi_{m'}\Psi_{n'}$$

$$+ c_{\text{dd}}\sum_{\mu=x,y,z}\sum_{n=-F}^{F} b_\mu(F_\mu)_{mn}\Psi_n, \quad (1)$$

where $\Psi_m(\boldsymbol{r},t)$ is the condensate wave function for the atoms in the magnetic sublevel m and $H_0 = -\hbar^2\nabla^2/(2M) + U_{\text{trap}}(\boldsymbol{r})$, with M being the atomic mass and U_{trap} the spin-independent trapping potential. The linear and quadratic Zeeman energies per atom are given by $p = g_F\mu_B B$ and $q = (g_F\mu_B B)^2/E_{\text{hf}}$, respectively, where g_F is the hyperfine g-factor, μ_B is the Bohr magneton, and E_{hf} is the hyperfine energy splitting. The second term on the right-hand side of Eq. (1) comes from

the short-range part of the two-body interaction given by

$$V_s(\boldsymbol{r},\boldsymbol{r}') = \delta(\boldsymbol{r}-\boldsymbol{r}') \sum_{S=0,\text{even}}^{2F} \frac{4\pi\hbar^2}{M} a_S \mathcal{P}_S, \quad (2)$$

where $\mathcal{P}_S = \sum_{M_S=-S}^{S} |SM_S\rangle\langle SM_S|$ projects a pair of spin-1 atoms into the state with total spin S, and a_S is the s-wave scattering length for the corresponding spin channel S. The scattering amplitude for odd S vanishes due to Bose symmetrization, and $\langle mn|SM_S\rangle$ in Eq. (1) is the Clebsch-Gordan coefficient. The last term on the right-hand side of Eq. (1) corresponds to the MDDI, where $c_{\text{dd}} = \mu_0(g_F\mu_B)^2/(4\pi)$, with μ_0 being the magnetic permeability of the vacuum. Here, we define the nonlocal dipole field by

$$b_\mu(\boldsymbol{r}) = \int d^3r' \sum_\nu Q_{\mu\nu}(\boldsymbol{r}-\boldsymbol{r}')f_\nu(\boldsymbol{r}'), \quad (3)$$

where $Q_{\mu\nu}(\boldsymbol{r})$ is the dipole kernel, given in Sec. II C, and

$$f_\mu = \sum_{mn} \Psi_m^*(F_\mu)_{mn}\Psi_n \quad (4)$$

is the spin density, with $F_{x,y,z}$ being the spin-F matrices. Below we omit the summation symbol: Greek indices that appear twice are to be summed over x, y, and z, and Roman indices are to be summed over $-F, \ldots, F$.

From the GP equation, we can immediately derive the mass continuity equation:

$$\frac{\partial n_{\text{tot}}}{\partial t} + \boldsymbol{\nabla}\cdot(n_{\text{tot}}\boldsymbol{v}_{\text{mass}}) = 0, \quad (5)$$

where

$$n_{\text{tot}} = \Psi_m^*\Psi_m, \quad (6)$$

$$n_{\text{tot}}\boldsymbol{v}_{\text{mass}} = \frac{\hbar}{2Mi}[\Psi_m^*(\boldsymbol{\nabla}\Psi_m) - (\boldsymbol{\nabla}\Psi_m^*)\Psi_m] \quad (7)$$

are the number density and superfluid current, respectively. By introducing a normalized spinor ζ_m defined by $\Psi_m(\boldsymbol{r},t) = \sqrt{n_{\text{tot}}(\boldsymbol{r},t)}\zeta_m(\boldsymbol{r},t)$, the superfluid velocity $\boldsymbol{v}_{\text{mass}}$ can be written as

$$\boldsymbol{v}_{\text{mass}} = \frac{\hbar}{2Mi}[\zeta_m^*(\boldsymbol{\nabla}\zeta_m) - (\boldsymbol{\nabla}\zeta_m^*)\zeta_m]. \quad (8)$$

In the absence of the linear and quadratic Zeeman effects and the MDDI, the continuity equation of the spin density can also be derived from the GP equation as

$$\frac{\partial f_\mu}{\partial t} + \boldsymbol{\nabla}\cdot(n_{\text{tot}}\boldsymbol{v}_{\text{spin}}^\mu) = 0, \quad (9)$$

where $\boldsymbol{v}_{\text{spin}}^\mu$ is the spin superfluid velocity defined by

$$\boldsymbol{v}_{\text{spin}}^\mu = \frac{\hbar}{2Mi}(F_\mu)_{mn}[\zeta_m^*(\boldsymbol{\nabla}\zeta_n) - (\boldsymbol{\nabla}\zeta_m^*)\zeta_n]. \quad (10)$$

The short-range interaction does not contribute to the equation of motion of spin, since it conserves the total spin of two colliding atoms. The detailed calculation is given in the Appendix. In the presence of the external magnetic field along the z direction, the linear Zeeman effect induces a torque term $(p/\hbar)(\hat{z}\times\boldsymbol{f})_\mu$ on the right-hand side of Eq. (9), which causes the precession of spins. In a similar manner, the dipole field also induces a torque term $(c_{\text{dd}}/\hbar)(\boldsymbol{b}\times\boldsymbol{f})_\mu$. On the other hand, the quadratic Zeeman term does not conserve the transverse

magnetization, and its effect is written as $(2q/\hbar)\epsilon_{\mu z\nu}n_{\text{tot}}\hat{\mathcal{N}}_{z\nu}$, where ϵ_{ijk} is the Levi-Civita symbol, and

$$\hat{\mathcal{N}}_{\mu\nu} = \tfrac{1}{2}\zeta_m^*(F_\mu F_\nu + F_\nu F_\mu)_{mn}\zeta_n \quad (11)$$

is a nematic tensor. The derivations of these three terms are given in the Appendix. As a result, we obtain the equation of motion of spins in the presence of the MDDI and linear and quadratic Zeeman effects under the external field parallel to the z axis:

$$\frac{\partial f_\mu}{\partial t} + \boldsymbol{\nabla}\cdot(n_{\text{tot}}\boldsymbol{v}_{\text{spin}}^\mu) = \frac{c_{\text{dd}}}{\hbar}(\boldsymbol{b}\times\boldsymbol{f})_\mu + \frac{p}{\hbar}(\hat{z}\times\boldsymbol{f})_\mu$$
$$+ \frac{2q}{\hbar}n_{\text{tot}}\epsilon_{\mu z\nu}\hat{\mathcal{N}}_{z\nu}. \quad (12)$$

Equations (5) and (12) hold in all phases, independent of scattering length.

B. Ferromagnetic BEC

In the following, we consider a ferromagnetic BEC. We assume that the BEC is fully magnetized, $|\boldsymbol{f}| = Fn_{\text{tot}}$, and only the direction of the spin density can vary in space. This assumption is valid when the ferromagnetic interaction energy is large enough compared with the other spinor interaction energies, MDDI energy, quadratic Zeeman energy, and the kinetic energy arising from the spacial variation of the direction of $\boldsymbol{f}$. The linear Zeeman effect is not necessarily weaker than the ferromagnetic interaction, since it merely induces the Larmor precession. For example, the short-range interaction (2) for a spin-1 BEC can be written as [20]

$$\langle mn|V_s(\boldsymbol{r},\boldsymbol{r}')|m'n'\rangle$$
$$= \delta(\boldsymbol{r}-\boldsymbol{r}')[c_0\delta_{mn}\delta_{m'n'} + c_1(F_\mu)_{mn}(F_\mu)_{m'n'}], \quad (13)$$

where $c_0 = 4\pi\hbar^2(2a_2+a_0)/(3M)$ and $c_1 = 4\pi\hbar^2(a_2-a_0)/(3M)$. The ground state is ferromagnetic for $c_1 < 0$. The above assumption is valid when $q \ll |c_1|n_{\text{tot}}$, $c_{\text{dd}} \ll |c_1|$, and the length scale of the spatial spin structure is larger than the spin healing length $\xi_{\text{sp}} = \hbar/\sqrt{2M|c_1|n_{\text{tot}}}$. Moreover, in the incompressible limit, namely, when the spin-independent interaction (c_0n_{tot} for the case of a spin-1 BEC) is much stronger than the ferromagnetic interaction and MDDI, the number density n_{tot} is determined regardless of the spin structure and assumed to be stationary. This is the case for the spin-1 ^{87}Rb BEC.

We then rewrite the equations of motion (5) and (12) in terms of a unit vector $\hat{\boldsymbol{f}} \equiv \boldsymbol{f}/(Fn_{\text{tot}})$ that describes the direction of the spin density and the superfluid velocity $\boldsymbol{v}_{\text{mass}}$ defined in Eq. (8). The order parameter for the spin-polarized state in the z direction is given by $\zeta_m^{(0)} = \delta_{mF}$. The general order parameter is obtained by performing the gauge transformation and Euler rotation as

$$\boldsymbol{\zeta} = e^{i\phi}e^{-iF_z\alpha}e^{-iF_y\beta}e^{-iF_z\gamma}\boldsymbol{\zeta}^{(0)}$$
$$= e^{i(\phi-F\gamma)}e^{-iF_z\alpha}e^{-iF_y\beta}\boldsymbol{\zeta}^{(0)}, \quad (14)$$

where α, β, and γ are Euler angles shown in Fig. 1 and ϕ is the overall phase. Due to the spin-gauge symmetry of the ferromagnetic BEC, i.e., the equivalence between the phase change ϕ and spin rotation γ, distinct configurations of $\boldsymbol{\zeta}$ are characterized with a set of parameters $(\alpha, \beta, \phi' \equiv \phi - F\gamma)$. Here, α and β denote the direction of $\hat{\boldsymbol{f}}$ as shown in Fig. 1.
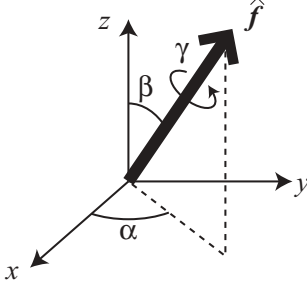
FIG. 1. Euler rotation of the unit vector $\hat{\boldsymbol{f}}$.

Actually, $\hat{\boldsymbol{f}}$ for the order parameter (14) is calculated as

$$
\begin{aligned}
F\hat{\boldsymbol{f}} &= \zeta_m^* \boldsymbol{F}_{mn} \zeta_n \\
&= \zeta_m^{(0)*} (e^{iF_y\beta} e^{iF_z\alpha} \boldsymbol{F} e^{-iF_z\alpha} e^{-iF_y\beta})_{mn} \zeta_n^{(0)} \\
&= \mathcal{R}_z(\alpha)\mathcal{R}_y(\beta) \left[\zeta_m^{(0)*} \boldsymbol{F}_{mn} \zeta_n^{(0)} \right] \\
&= F \begin{pmatrix} \sin\beta\cos\alpha \\ \sin\beta\sin\alpha \\ \cos\beta \end{pmatrix},
\end{aligned} \tag{15}
$$

where $\mathcal{R}_z(\alpha)$ and $\mathcal{R}_y(\beta)$ are the 3×3 matrices describing the rotation about the z axis by α and about the y axis by β, respectively. In a similar manner, we obtain the nematic tensor $\hat{\mathcal{N}}$ for the order parameter (14) as

$$
\begin{aligned}
\hat{\mathcal{N}}_{\mu\nu} &= \mathcal{R}_z(\alpha)\mathcal{R}_y(\beta)\hat{\mathcal{N}}_{\mu\nu}^{(0)}\mathcal{R}_y^T(\beta)\mathcal{R}_z^T(\alpha) \\
&= \frac{F}{2}\delta_{\mu\nu} + \frac{F(2F-1)}{2}\hat{f}_\mu\hat{f}_\nu,
\end{aligned} \tag{16}
$$

where T denotes the transpose and $\hat{\mathcal{N}}_{\mu\nu}^{(0)} = \frac{1}{2}\zeta_m^{(0)*}(F_\mu F_\nu + F_\nu F_\mu)_{mn}\zeta_n^{(0)}$ is the nematic tensor for $\boldsymbol{\zeta}^{(0)}$, which is given by

$$
\begin{aligned}
\hat{\mathcal{N}}^{(0)} &= \begin{pmatrix} F/2 & 0 & 0 \\ 0 & F/2 & 0 \\ 0 & 0 & F^2 \end{pmatrix} \\
&= \frac{F}{2}\begin{pmatrix} 1 & 0 & 0 \\ 0 & 1 & 0 \\ 0 & 0 & 1 \end{pmatrix} + \frac{F(2F-1)}{2}\begin{pmatrix} 0 & 0 & 0 \\ 0 & 0 & 0 \\ 0 & 0 & 1 \end{pmatrix}.
\end{aligned} \tag{17}
$$

Substituting Eq. (14) and

$$
\nabla\zeta = i[\nabla\phi' - (\nabla\alpha)F_z - (\nabla\beta)e^{-iF_z\alpha}F_y e^{iF_z\alpha}]\zeta \tag{18}
$$

into Eq. (8), the superfluid velocity can be written as

$$
\boldsymbol{v}_{\text{mass}} = \frac{\hbar}{M}[\nabla\phi' - F(\nabla\alpha)\cos\beta], \tag{19}
$$

which satisfies the Mermin-Ho relation [21]:

$$
\nabla\times\boldsymbol{v}_{\text{mass}} = \frac{\hbar F}{2M}\epsilon_{\mu\nu\lambda}\hat{f}_\mu(\nabla\hat{f}_\nu\times\nabla\hat{f}_\lambda). \tag{20}
$$

As we mentioned before, n_{tot} is stationary in the incompressible limit. Thus, Eq. (5) becomes

$$
\nabla\cdot(n_{\text{tot}}\boldsymbol{v}_{\text{mass}}) = 0. \tag{21}
$$

Equations (20) and (21) are equations for the superfluid velocity. Next, we consider the equation for the spin superfluid velocity. Making use of Eq. (16), Eq. (10) can be rewritten in terms of $\hat{\boldsymbol{f}}$ and $\boldsymbol{v}_{\text{mass}}$ as

$$
\begin{aligned}
\boldsymbol{v}_{\text{spin}}^\mu &= \frac{\hbar}{M}[(\nabla\phi')F\hat{f}_\mu - (\nabla\alpha)\hat{\mathcal{N}}_{\mu z} - (\nabla\beta)\hat{\mathcal{N}}_{\mu y}\cos\alpha + (\nabla\beta)\hat{\mathcal{N}}_{\mu x}\sin\alpha] \\
&= F\hat{f}_\mu\boldsymbol{v}_{\text{mass}} - \frac{\hbar F}{2M}\left[(\nabla\alpha)\sin\beta\begin{pmatrix} -\cos\beta\cos\alpha \\ -\cos\beta\sin\alpha \\ \sin\beta \end{pmatrix} + (\nabla\beta)\begin{pmatrix} -\sin\alpha \\ \cos\alpha \\ 0 \end{pmatrix}\right]_\mu \\
&= F\hat{f}_\mu\boldsymbol{v}_{\text{mass}} - \frac{\hbar F}{2M}\epsilon_{\mu\nu\lambda}\hat{f}_\nu\nabla\hat{f}_\lambda.
\end{aligned} \tag{22}
$$

Substituting Eqs. (16), (21), and (22) into Eq. (12), we obtain the hydrodynamic equation in terms of $\hat{\boldsymbol{f}}$ and $\boldsymbol{v}_{\text{mass}}$ as

$$
\frac{\partial\hat{\boldsymbol{f}}}{\partial t} + (\boldsymbol{v}_{\text{mass}}\cdot\nabla)\hat{\boldsymbol{f}} = -\hat{\boldsymbol{f}}\times\boldsymbol{B}_{\text{eff}}, \tag{23}
$$

with

$$
\begin{aligned}
\boldsymbol{B}_{\text{eff}} = &-\frac{\hbar}{2M}(\boldsymbol{a}\cdot\nabla)\hat{\boldsymbol{f}} - \frac{\hbar}{2M}\nabla^2\hat{\boldsymbol{f}} + \frac{c_{\text{dd}}}{\hbar}\boldsymbol{b} + \frac{p}{\hbar}\hat{e}^B \\
&+ \frac{q(2F-1)}{\hbar}(\hat{e}^B\cdot\hat{\boldsymbol{f}})\hat{e}^B,
\end{aligned}
$$

where $\boldsymbol{a} = (\nabla n_{\text{tot}})/n_{\text{tot}}$ and $\hat{e}^B$ is the unit vector along the external field ($\hat{e}^B = \hat{z}$ in this paper). Here we note that Eq. (23) has the same form as the extended Landau-Lifshitz-Gilbert

equation (without damping) which includes the adiabatic spin torque term [22].

C. Quasi-2D system

We next consider a quasi-2D system, that is, we consider a BEC confined in a quasi-2D trap whose Thomas-Fermi radius in the normal direction to the 2D plane is smaller than the spin healing length. We approximate the wave function in the normal direction by a Gaussian with width d: $\Psi_m(\boldsymbol{r}_\perp, r_n) = \psi_m(\boldsymbol{r}_\perp)h(r_n)$, where $\boldsymbol{r}_\perp$ is the position vector in the 2D plane, r_n is the coordinate in the normal direction, and $h(r_n) = \exp[-r_n^2/(4d^2)]/(2\pi d^2)^{1/4}$. Multiplying the wave function to Eq. (1) and integrating over r_n, we obtain the 2D GP equation. The equation is the same as Eq. (1) if one replaces Ψ_m with ψ_m, a_S with ηa_S, c_{dd} with ηc_{dd}, and $\boldsymbol{b}$ with

$\bar{\boldsymbol{b}}$, where $\eta = \int dr_n h^4(r_n) / \int dr_n h^2(r_n) = 1/\sqrt{4\pi d^2}$ and

$$\bar{b}_\mu = \int d^2 r'_\perp Q^{(2D)}_{\mu\nu}(\boldsymbol{r}_\perp - \boldsymbol{r}'_\perp)[\psi^*_m(\boldsymbol{r}'_\perp)(F_\nu)_{mn}\psi_n(\boldsymbol{r}'_\perp)], \quad (24)$$

with

$$Q^{(2D)}_{\mu\nu}(\boldsymbol{r}_\perp - \boldsymbol{r}'_\perp) = \frac{1}{\eta} \iint dr_n dr'_n h^2(r_n) h^2(r'_n) Q_{\mu\nu}(\boldsymbol{r} - \boldsymbol{r}'). \quad (25)$$

Starting from the 2D GP equation and following the above procedure, we derive the 2D hydrodynamic equation:

$$\frac{\partial \hat{\boldsymbol{f}}}{\partial t} + (\boldsymbol{v}_{\text{mass}} \cdot \nabla)\hat{\boldsymbol{f}} = -\hat{\boldsymbol{f}} \times \bar{\boldsymbol{B}}_{\text{eff}}, \quad (26)$$

with

$$\begin{aligned}
\bar{\boldsymbol{B}}_{\text{eff}} = &-\frac{\hbar}{2M}(\boldsymbol{a} \cdot \nabla)\hat{\boldsymbol{f}} - \frac{\hbar}{2M}\nabla^2 \hat{\boldsymbol{f}} + \frac{\eta c_{\text{dd}}}{\hbar}\bar{\boldsymbol{b}} + \frac{p}{\hbar}\hat{e}^B \\
&+ \frac{q(2F-1)}{\hbar}(\hat{e}^B \cdot \hat{\boldsymbol{f}})\hat{e}^B,
\end{aligned}$$

where $\boldsymbol{v}_{\text{mass}}$ and ∇ are the two-dimensional vector and vector operator, respectively. When we consider a quasi-2D BEC, n_{tot}, $\hat{\boldsymbol{f}}$, and $\boldsymbol{v}_{\text{mass}}$ are defined by means of ψ_m instead of Ψ_m.

D. Dipole kernel

This section provides the detailed form of the dipole kernel in three-dimensional (3D) and quasi-2D systems under zero external field and under a strong magnetic field ($p \gg c_{\text{dd}}n_{\text{tot}}$). The derivations are given in Ref. [15].

The dipole kernel in the laboratory frame of reference is given by

$$Q^{(\text{lab})}_{\mu\nu}(\boldsymbol{r}) = \frac{\delta_{\mu\nu} - 3\hat{r}_\mu \hat{r}_\nu}{r^3}, \quad (27)$$

with $r = |\boldsymbol{r}|$ and $\hat{\boldsymbol{r}} = \boldsymbol{r}/r$. The 2D dipole kernel in the laboratory frame is calculated by substituting Eq. (27) into Eq. (25). For $\boldsymbol{r}_\perp = (x,y)$ and $r_n = z$, the 2D dipole kernel is given by

$$Q^{(2D,\text{lab})}_{\mu\nu}(\boldsymbol{r}_\perp) = \sum_{\boldsymbol{k}_\perp} e^{i\boldsymbol{k}_\perp \cdot \boldsymbol{r}_\perp} \tilde{Q}^{(2D,\text{lab})}_{\boldsymbol{k}_\perp \mu\nu}, \quad (28)$$

where

$$\begin{aligned}
\tilde{Q}^{(2D,\text{lab})}_{\boldsymbol{k}_\perp} = &-\frac{4\pi}{3}\begin{pmatrix} 1 & 0 & 0 \\ 0 & 1 & 0 \\ 0 & 0 & -2 \end{pmatrix} \\
&+ 4\pi G(k_\perp d)\begin{pmatrix} \hat{k}_x^2 & \hat{k}_x \hat{k}_y & 0 \\ \hat{k}_x \hat{k}_y & \hat{k}_y^2 & 0 \\ 0 & 0 & -1 \end{pmatrix}, \quad (29)
\end{aligned}$$

with $\boldsymbol{k}_\perp = (k_x, k_y)$, $k_\perp = |\boldsymbol{k}_\perp|$, $\hat{k}_{x,y} = k_{x,y}/k_\perp$, and $G(k) \equiv 2ke^{k^2}\int_k^\infty e^{-t^2}dt = \sqrt{\pi}ke^{k^2}\text{erfc}(k)$. It can be shown that $G(k)$ is a monotonically increasing function that satisfies $G(0) = 0$ and $G(\infty) = 1$.

When the linear Zeeman energy is much larger than the MDDI energy, we choose the rotating frame of reference in spin space by replacing Ψ_m with $e^{-ipmt/\hbar}\Psi_m$, and eliminate the linear Zeeman term from the GP equation. In this case, the contribution of the MDDI is time-averaged due to the Larmor precession, and we use the dipole kernel which is averaged over the Larmor precession period given by [23]

$$Q^{(\text{rot})}_{\mu\nu}(\boldsymbol{r}) = -\frac{1}{2}\frac{1 - 3\hat{r}_z^2}{r^3}(\delta_{\mu\nu} - 3\delta_{z\mu}\delta_{z\nu}). \quad (30)$$

Substituting Eq. (30) into Eq. (25), we obtain the time-averaged 2D dipole kernel in the rotating frame as

$$Q^{(2D,\text{rot})}_{\mu\nu}(\boldsymbol{r}_\perp) = (\delta_{\mu\nu} - 3\delta_{z\mu}\delta_{z\nu})\sum_{\boldsymbol{k}_\perp} e^{i\boldsymbol{k}_\perp \cdot \boldsymbol{r}_\perp} \tilde{Q}_{\boldsymbol{k}_\perp}, \quad (31)$$

where

$$\tilde{Q}_{\boldsymbol{k}_\perp} = \frac{2\pi}{3}\{1 - 3(\hat{e}_n \cdot \hat{e}^B)^2 - 3G(k_\perp d)[(\hat{e}^B_\perp \cdot \hat{\boldsymbol{k}}_\perp)^2 - (\hat{e}_n \cdot \hat{e}^B)^2]\}. \quad (32)$$

Here, $\hat{\boldsymbol{k}}_\perp = \boldsymbol{k}_\perp/k_\perp$, $\hat{e}_n$ is the unit vector normal to the plane, and $\hat{e}^B_\perp$ is the vector of $\hat{e}^B$ projected onto the 2D plane.

E. Stereographic projection

The spin dynamics are now described by Eqs. (20), (21), and (23) or (26). We rewrite the equations by means of stereographic projection [24]: we employ a complex number $\varphi = (\hat{f}_x + i\hat{f}_y)/(1 + \hat{f}_z)$ to express the spin variables,

$$\hat{f}_x = \frac{\varphi + \varphi^*}{1 + \varphi\varphi^*}, \quad \hat{f}_y = \frac{-i(\varphi - \varphi^*)}{1 + \varphi\varphi^*}, \quad \hat{f}_z = \frac{1 - \varphi\varphi^*}{1 + \varphi\varphi^*}. \quad (33)$$

Equation (20) is rewritten as

$$\nabla \times \boldsymbol{v}_{\text{mass}} = iF\frac{2\hbar}{M}\frac{\nabla\varphi \times \nabla\varphi^*}{(1 + \varphi\varphi^*)^2}, \quad (34)$$

while Eq. (21) remains the same. In order to rewrite the equation of spins, we need to specify the dimensionality of the system and the direction and strength of the external field. In this paper, we consider the following two cases: (i) a quasi-2D system normal to the z axis under zero magnetic field, and (ii) a quasi-2D system normal to the y axis with a strong magnetic field along the z axis. Case (ii) corresponds to the situation in the Berkeley experiment [9].

For case (i), we take $\hat{e}_n = \hat{z}$ and $p = q = 0$ and use Eqs. (24), (26), (28), and (29). Using the stereographic projection, the equation of motion of spins is given by

$$\begin{aligned}
\frac{\partial \varphi(\boldsymbol{r},t)}{\partial t} = &-\boldsymbol{v}_{\text{mass}} \cdot \nabla\varphi + \frac{i\hbar}{2Mn_{\text{tot}}}\nabla n_{\text{tot}} \cdot \nabla\varphi + \frac{i\hbar}{2M}\nabla^2\varphi - \frac{i\hbar}{M}\frac{\varphi^*(\nabla\varphi)^2}{1 + \varphi\varphi^*} \\
&- \frac{i\eta c_{\text{dd}}F}{2\hbar}\int d^2r' n_{\text{tot}}(\boldsymbol{r}')\sum_{\boldsymbol{k}} e^{i\boldsymbol{k}\cdot(\boldsymbol{r}-\boldsymbol{r}')}\left[-h_1(k)\frac{\varphi(\boldsymbol{r}')}{1 + \varphi(\boldsymbol{r}')\varphi^*(\boldsymbol{r}')} + h_2(k)\frac{\varphi^*(\boldsymbol{r}')}{1 + \varphi(\boldsymbol{r}')\varphi^*(\boldsymbol{r}')}\right]
\end{aligned}$$

$$+ \frac{i\eta c_{\text{dd}} F}{2\hbar} \varphi^2 \int d^2 r' n_{\text{tot}}(\boldsymbol{r}') \sum_{\boldsymbol{k}} e^{i\boldsymbol{k}\cdot(\boldsymbol{r}-\boldsymbol{r}')} \left[-h_1(k) \frac{\varphi^*(\boldsymbol{r}')}{1 + \varphi(\boldsymbol{r}')\varphi^*(\boldsymbol{r}')} + h_2^*(k) \frac{\varphi(\boldsymbol{r}')}{1 + \varphi(\boldsymbol{r}')\varphi^*(\boldsymbol{r}')} \right]$$

$$+ \frac{i\eta c_{\text{dd}} F}{\hbar} \varphi \int d^2 r' n_{\text{tot}}(\boldsymbol{r}') \sum_{\boldsymbol{k}} e^{i\boldsymbol{k}\cdot(\boldsymbol{r}-\boldsymbol{r}')} h_1(k) \frac{1 - \varphi(\boldsymbol{r}')\varphi^*(\boldsymbol{r}')}{1 + \varphi(\boldsymbol{r}')\varphi^*(\boldsymbol{r}')}, \tag{35}$$

where the subscript $\perp$ was omitted for simplicity and

$$h_1(k) = \frac{8\pi}{3} - 4\pi G(kd), \tag{36}$$

$$h_2(k) = 4\pi G(kd) (\hat{k}_x + i\hat{k}_y)^2. \tag{37}$$

For case (ii), we take $\hat{e}_{\text{n}} = \hat{y}$, $\hat{e}^B = \hat{z}$, and $p = 0$, and use Eqs. (24), (26), (31), and (32). Then, the equation of motion of spins is described as

$$\frac{\partial \varphi(\boldsymbol{r},t)}{\partial t} = -\boldsymbol{v}_{\text{mass}} \cdot \nabla \varphi + \frac{i\hbar}{2M n_{\text{tot}}} \nabla n_{\text{tot}} \cdot \nabla \varphi + \frac{i\hbar}{2M} \nabla^2 \varphi - \frac{i\hbar}{M} \frac{\varphi^*(\nabla \varphi)^2}{1 + \varphi\varphi^*} - \frac{i\eta c_{\text{dd}} F}{\hbar} \int d^2 r' n_{\text{tot}}(\boldsymbol{r}') \sum_{\boldsymbol{k}} e^{i\boldsymbol{k}\cdot(\boldsymbol{r}-\boldsymbol{r}')} \tilde{Q}_{\boldsymbol{k}} \frac{\varphi(\boldsymbol{r}')}{1 + \varphi(\boldsymbol{r}')\varphi^*(\boldsymbol{r}')}$$

$$+ \frac{i\eta c_{\text{dd}} F}{\hbar} \varphi^2 \int d^2 r' n_{\text{tot}}(\boldsymbol{r}') \sum_{\boldsymbol{k}} e^{i\boldsymbol{k}\cdot(\boldsymbol{r}-\boldsymbol{r}')} \tilde{Q}_{\boldsymbol{k}} \frac{\varphi^*(\boldsymbol{r}')}{1 + \varphi(\boldsymbol{r}')\varphi^*(\boldsymbol{r}')} - \frac{2i\eta c_{\text{dd}} F}{\hbar} \varphi \int d^2 r' n_{\text{tot}}(\boldsymbol{r}') \sum_{\boldsymbol{k}} e^{i\boldsymbol{k}\cdot(\boldsymbol{r}-\boldsymbol{r}')} \tilde{Q}_{\boldsymbol{k}} \frac{1 - \varphi(\boldsymbol{r}')\varphi^*(\boldsymbol{r}')}{1 + \varphi(\boldsymbol{r}')\varphi^*(\boldsymbol{r}')}$$

$$+ \frac{iq(2F - 1)}{\hbar} \frac{1 - \varphi\varphi^*}{1 + \varphi\varphi^*} \varphi, \tag{38}$$

where $\boldsymbol{r}_\perp \to \boldsymbol{r} = (x,z)$ and $\boldsymbol{k}_\perp \to \boldsymbol{k} = (k_x,k_z)$.

III. DYNAMICAL INSTABILITY

The hydrodynamic equations derived above give a rather straightforward approach to the analysis of the spin dynamics in a spinor BEC. In this section, we analyze the dynamical instability for cases (i) and (ii). Here we consider a uniform quasi-2D system and assume $\nabla n_{\text{tot}} = 0$.

A. Case (i): Instability under zero external field

Here we analyze the dynamical instability under zero external field for two initial stationary structures: uniform spin structures polarized normal to the x-y plane ($\varphi_0 = 0$) and in the x-y plane ($\varphi_0 = 1$).

First, we consider the case in which the spins are polarized normal to the x-y plane, i.e., in the z direction, $\varphi_0 = 0$. Substituting $\varphi = 0 + \delta\varphi$ and $\boldsymbol{v}_{\text{mass}} = \boldsymbol{v}_0 + \delta\boldsymbol{v}$ into Eq. (35), we obtain linearized equations of $\delta\varphi$ and $\delta\varphi^*$. Performing Fourier expansions $\delta\varphi = \sum_{\boldsymbol{k}} \delta\tilde{\varphi}_{\boldsymbol{k}} e^{i\boldsymbol{k}\cdot\boldsymbol{r}}$ and $\delta\varphi^* = \sum_{\boldsymbol{k}} \delta\tilde{\varphi}_{-\boldsymbol{k}}^* e^{i\boldsymbol{k}\cdot\boldsymbol{r}}$, we have

$$\frac{d}{dt} \begin{pmatrix} \delta\tilde{\varphi}_{\boldsymbol{k}} \\ \delta\tilde{\varphi}_{-\boldsymbol{k}}^* \end{pmatrix} = \frac{i}{\hbar} \begin{pmatrix} -g_0 - g_1 & -g_2 \\ g_2^* & -g_0 + g_1 \end{pmatrix} \begin{pmatrix} \delta\tilde{\varphi}_{\boldsymbol{k}} \\ \delta\tilde{\varphi}_{-\boldsymbol{k}}^* \end{pmatrix}, \tag{39}$$

where

$$g_0(\boldsymbol{k}) = \hbar \boldsymbol{v}_0 \cdot \boldsymbol{k}, \tag{40}$$

$$g_1(\boldsymbol{k}) = \frac{\hbar^2 k^2}{2M} - 2\pi \tilde{c}_{\text{dd}} [2 - G(kd)], \tag{41}$$

$$g_2(\boldsymbol{k}) = 2\pi \tilde{c}_{\text{dd}} G(kd) (\hat{k}_x + i\hat{k}_y)^2. \tag{42}$$

Here, $\tilde{c}_{\text{dd}} = \eta c_{\text{dd}} n_{\text{tot}} F$ and $\boldsymbol{k} = (k_x,k_y)$. The eigenvalues of the 2×2 matrix in Eq. (39) are

$$\lambda_\pm(\boldsymbol{k}) = -\frac{i}{\hbar} g_0 \pm \frac{1}{\hbar} \sqrt{|g_2|^2 - g_1^2}. \tag{43}$$

The system becomes dynamically unstable when one of the eigenvalues has a positive real part; that is when $\text{Re}\lambda_+(\boldsymbol{k}) > 0$ (or $|g_2|^2 - g_1^2 > 0$). The wave-vector dependence of $\text{Re}\lambda_+$ is shown in Fig. 2. When the BEC is polarized perpendicular to the 2D plane, the MDDI is repulsive and isotropic in the 2D plane. Thus, the BEC is unstable against spin flip, and the unstable modes distribute isotropically in the momentum
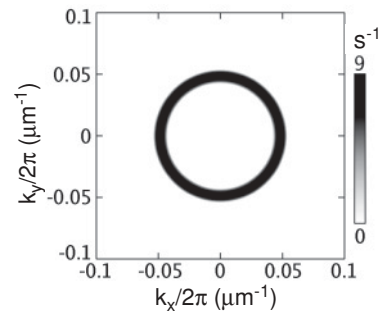

FIG. 2. $\text{Re}\lambda_+(\boldsymbol{k})$ of the uniform spin structure polarized in the z direction under zero external field. The fluctuations in the black region are dynamically unstable and grow exponentially. Here, n_{tot} is given by $\sqrt{2\pi d^2} n_{\text{3D}}$ with $n_{\text{3D}} = 2.3 \times 10^{14}$ cm^{-3} and $d = 1.0$ μm. The other parameters are given by the typical values for a spin-1 ^{87}Rb atom: $M = 1.44 \times 10^{-25}$ kg, $F = 1$, $g_F = -1/2$, and $E_{\text{hf}} = 6.835$ GHz $\times h$.

space. The unstable region in the momentum space has a ring shape. The radius and width of the ring are estimated as $k_0 = (2/\hbar)\sqrt{2\pi M \tilde{c}_{\text{dd}}}$ and $\Delta k \simeq (\sqrt{\pi}/8)k_0^2 d(4 - \sqrt{\pi}k_0 d)$, respectively, for $kd \ll 1$.

Next, we consider the uniform spin structure polarized in the x direction, $\varphi_0 = 1$. We obtain the linearized equations in a similar way to the above. Substituting $\varphi = 1 + \delta\varphi$ and $\boldsymbol{v}_{\text{mass}} = \boldsymbol{v}_0 + \delta\boldsymbol{v}$ into Eq. (35) and performing the Fourier expansion, we obtain the equation of the same form as Eq. (39) with

$$g_0(\boldsymbol{k}) = \hbar \boldsymbol{v}_0 \cdot \boldsymbol{k}, \tag{44}$$

$$g_1(\boldsymbol{k}) = \frac{\hbar^2 k^2}{2M} + 2\pi \tilde{c}_{\text{dd}}\big[1 - G(kd)\big(1 - \hat{k}_y^2\big)\big], \tag{45}$$

$$g_2(\boldsymbol{k}) = 2\pi \tilde{c}_{\text{dd}}\big[1 - G(kd)\big(1 + \hat{k}_y^2\big)\big]. \tag{46}$$

In this case, it can be shown that $g_2^2 - g_1^2$ is always negative. Then, the eigenvalues which are given by the same form as Eq. (43) are purely imaginary regardless of $\boldsymbol{k}$. Hence, the spin-polarized state along the 2D plane is stable under zero magnetic field.

B. Case (ii): Instability under a strong magnetic field

Here we analyze the dynamical instability for the helical spin structure, $\varphi_0 = e^{i(\boldsymbol{\kappa}_\alpha \cdot \boldsymbol{r} - \omega_\alpha t)}$, characterized by the helix wave vector $\boldsymbol{\kappa}_\alpha$ in the x-z plane under a strong magnetic field in the z direction. Substituting $\varphi = \varphi_0$ and $\boldsymbol{v}_{\text{mass}} = \boldsymbol{v}_0$ into Eq. (38) gives $\omega_\alpha = \boldsymbol{v}_0 \cdot \boldsymbol{\kappa}_\alpha$. Substituting $\varphi = \varphi_0(1 + \delta\varphi)$ and $\boldsymbol{v}_{\text{mass}} = \boldsymbol{v}_0 + \delta\boldsymbol{v}$ into Eqs. (21) and (34), and holding the terms up to the first order of the fluctuations, we have $\nabla \cdot \boldsymbol{v}_0 = 0$, $\nabla \cdot \delta\boldsymbol{v} = 0$, $\nabla \times \boldsymbol{v}_0 = 0$, and $\nabla \times \delta\boldsymbol{v} = \frac{\hbar}{2M}(\nabla\delta\varphi + \nabla\delta\varphi^*) \times \boldsymbol{\kappa}_\alpha$. After Fourier expansions of $\delta\varphi$, $\delta\varphi^*$ and $\delta\boldsymbol{v} = \sum_{\boldsymbol{k}} \delta\tilde{\boldsymbol{v}}_{\boldsymbol{k}} e^{i\boldsymbol{k}\cdot\boldsymbol{r}}$, we have

$$\delta\tilde{\boldsymbol{v}}_{\boldsymbol{k}} = \frac{\hbar}{2M}(\delta\tilde{\varphi}_{\boldsymbol{k}} + \delta\tilde{\varphi}_{-\boldsymbol{k}}^*)\left[\boldsymbol{\kappa}_\alpha - \frac{(\boldsymbol{k}\cdot\boldsymbol{\kappa}_\alpha)\boldsymbol{k}}{k^2}\right]. \tag{47}$$

Substituting $\varphi = \varphi_0(1 + \delta\varphi)$ into Eq. (38) and applying Eq. (47), we obtain an equation of the same form as Eq. (39) with

$$g_0(\boldsymbol{k}) = \hbar \boldsymbol{v}_0 \cdot \boldsymbol{k}, \tag{48}$$

$$\begin{aligned} g_1(\boldsymbol{k}) = {} & \frac{\hbar^2 k^2}{2M} + \frac{\hbar^2}{2M}\left[\frac{\kappa_\alpha^2}{2} - \frac{(\boldsymbol{k}\cdot\boldsymbol{\kappa}_\alpha)^2}{k^2}\right] \\ & + \frac{\tilde{c}_{\text{dd}}}{4}(\tilde{\mathcal{Q}}_{\boldsymbol{k}+\boldsymbol{\kappa}_\alpha} + \tilde{\mathcal{Q}}_{\boldsymbol{k}-\boldsymbol{\kappa}_\alpha}) - \tilde{c}_{\text{dd}}(\tilde{\mathcal{Q}}_{\boldsymbol{\kappa}_\alpha} + \tilde{\mathcal{Q}}_{\boldsymbol{k}}) \\ & + \frac{q(2F-1)}{2}, \end{aligned} \tag{49}$$

$$\begin{aligned} g_2(\boldsymbol{k}) = {} & \frac{\hbar^2}{2M}\left[\frac{\kappa_\alpha^2}{2} - \frac{(\boldsymbol{k}\cdot\boldsymbol{\kappa}_\alpha)^2}{k^2}\right] - \frac{\tilde{c}_{\text{dd}}}{4}(\tilde{\mathcal{Q}}_{\boldsymbol{k}+\boldsymbol{\kappa}_\alpha} + \tilde{\mathcal{Q}}_{\boldsymbol{k}-\boldsymbol{\kappa}_\alpha}) \\ & - \tilde{c}_{\text{dd}}\tilde{\mathcal{Q}}_{\boldsymbol{k}} + \frac{q(2F-1)}{2}. \end{aligned} \tag{50}$$

Here, $\boldsymbol{k} = (k_x, k_z)$ and the Fourier transform of the dipole kernel is now simply given by $\tilde{\mathcal{Q}}_{\boldsymbol{k}} = (2\pi/3)[1 - 3(k_z/k)^2 G(kd)]$. The eigenvalues of the 2×2 matrix in Eq. (39) are given by Eq. (43) with Eqs. (48)–(50). When $\boldsymbol{\kappa}_\alpha \parallel \hat{z}$, $\boldsymbol{v}_0 = 0$, and neither the MDDI nor the quadratic Zeeman effect exist ($\tilde{c}_{\text{dd}} = q = 0$), the eigenvalues coincide with the dispersion relation derived in Ref. [17].

Figure 3 illustrates the wave-number dependence of $\text{Re}\lambda_+(\boldsymbol{k})$ for uniform and helical spin structures under various magnetic field strengths, indicating the region of dynamically unstable modes. The dynamical instability discussed here agrees qualitatively with that obtained by the Bogoliubov analysis [15,25]. However, there is a quantitative discrepancy in the magnetic field dependence of unstable modes caused by the fact that the local magnetization of the condensate is assumed to be fully polarized in our method. However, when q is not sufficiently small compared with the ferromagnetic interaction, the amplitude of the magnetization decreases as q increases. For the parameters used in the calculation for Fig. 3, our assumption is valid for $B \ll 480$ mG.
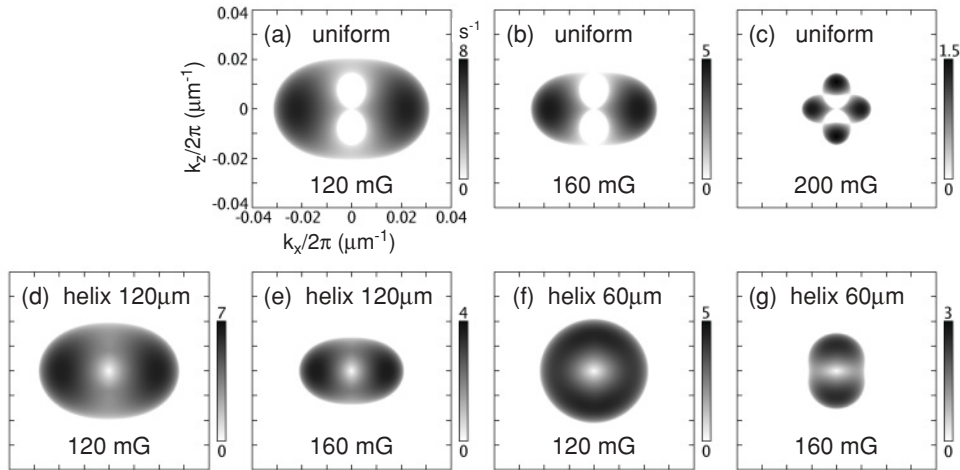

FIG. 3. $\text{Re}\lambda_+(\boldsymbol{k})$ for (a)–(c) uniform spin structures and (d)–(g) spin helices in the z direction with a pitch $2\pi/\kappa_\alpha$ under a strong magnetic field. The helical pitch for (d) and (e) is 120 μm, and that for (f) and (g) is 60 μm. The external field B is [(a), (d), and (f)] 120 mG, [(b), (e), and (g)] 160 mG, and (c) 200 mG. The other parameters are the same as those in Fig. 2.

IV. MAGNETIC FLUCTUATION PREFERENCE

We also investigate the magnetic fluctuation preference for two cases, that of dynamical instability under zero field for the uniform spin structure polarized normal to the x-y plane ($\varphi_0 = 0$), which is discussed in Sec. III A, and that of dynamical instability under a strong magnetic field for the helical spin structure ($\varphi_0 = e^{i(\kappa_\alpha \cdot r - \omega_\alpha t)}$), which is discussed in Sec. III B.

For the case of zero external field for $\varphi_0 = 0$, two kinds of magnetic fluctuations are considered: the x-direction fluctuation $\delta \hat{f}_x$ and the y-direction fluctuation $\delta \hat{f}_y$. They are described by the first order of $\delta\varphi$ as $\delta \hat{f}_x = 2\text{Re}(\delta\varphi)$ and $\delta \hat{f}_y = 2\text{Im}(\delta\varphi)$. Namely, the x- and y-direction fluctuations are characterized by the real and imaginary parts of $\delta\varphi$, respectively.

Let us reconsider the Fourier expansion of $\delta\varphi$,

$$
\begin{aligned}
\delta\varphi &= \frac{1}{2}\sum_{k \neq 0}(\delta\tilde{\varphi}_k e^{ik\cdot r} + \delta\tilde{\varphi}_{-k}e^{-ik\cdot r}) + \delta\tilde{\varphi}_0 \\
&= \frac{1}{2}\sum_{k \neq 0}[A_R\sin(k\cdot r + \alpha_R) + iA_I\sin(k\cdot r + \alpha_I)] + \delta\tilde{\varphi}_0,
\end{aligned}
$$
(51)

where

$$A_R = \sqrt{[\text{Re}(\delta\tilde{\varphi}_k + \delta\tilde{\varphi}_{-k})]^2 + [\text{Im}(\delta\tilde{\varphi}_k - \delta\tilde{\varphi}_{-k})]^2}, \quad (52)$$

$$A_I = \sqrt{[\text{Im}(\delta\tilde{\varphi}_k + \delta\tilde{\varphi}_{-k})]^2 + [\text{Re}(\delta\tilde{\varphi}_k - \delta\tilde{\varphi}_{-k})]^2}, \quad (53)$$

and $\alpha_R = \tan^{-1}[\text{Re}(\delta\tilde{\varphi}_k + \delta\tilde{\varphi}_{-k})/\text{Im}(\delta\tilde{\varphi}_{-k} - \delta\tilde{\varphi}_k)]$ and $\alpha_I = \tan^{-1}[\text{Im}(\delta\tilde{\varphi}_k + \delta\tilde{\varphi}_{-k})/\text{Re}(\delta\tilde{\varphi}_k - \delta\tilde{\varphi}_{-k})]$. As $\lambda_+(k = 0) = 0$, $\delta\tilde{\varphi}_0 = 0$. We introduce the quantity θ, which characterizes the magnetic fluctuation preference:

$$\theta = \tan^{-1}(A_R/A_I). \quad (54)$$

Here, we calculate $\theta(k)$ for the unstable modes shown in Fig. 2. The eigenvector which corresponds to the eigenvalue λ_+ of the 2×2 matrix in Eq. (39) is given by

$$\begin{pmatrix} \delta\tilde{\varphi}_k \\ \delta\tilde{\varphi}_{-k}^* \end{pmatrix} = \begin{pmatrix} (g_1 + i\sqrt{|g_2|^2 - g_1^2})/\sqrt{2|g_2|^2} \\ -g_2^*/\sqrt{2|g_2|^2} \end{pmatrix}, \quad (55)$$
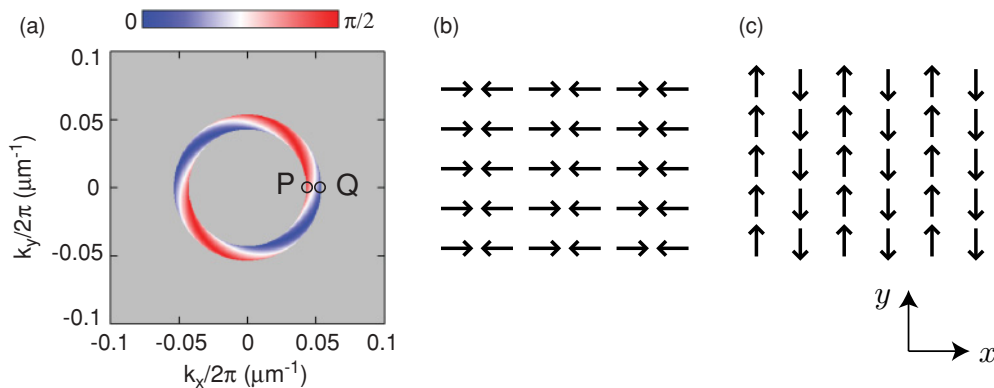
where g_1 and g_2 are defined by Eqs. (41) and (42), respectively. Then, from Eqs. (52)–(55), we obtain

$$\theta(k) = \tan^{-1}\left[\frac{|g_2|^2 - g_1\text{Re}(g_2) + \text{Im}(g_2)\sqrt{|g_2|^2 - g_1^2}}{|g_2|^2 + g_1\text{Re}(g_2) - \text{Im}(g_2)\sqrt{|g_2|^2 - g_1^2}}\right]^{1/2}. \quad (56)$$

We can consider the x-direction fluctuation to be dominant for $\pi/4 < \theta < \pi/2$ and the y-direction fluctuation to be dominant for $0 < \theta < \pi/4$.

The wave-vector dependence of $\theta(k)$ for the unstable mode shown in Fig. 2 is illustrated in Fig. 4(a). In the red (blue) regions, the $x(y)$-direction fluctuation is more dominant than the $y(x)$-direction fluctuation. The schematic pictures of the magnetic patterns induced by the dynamical instability at points P and Q are illustrated in Figs. 4(b) and 4(c), respectively. At point P in Fig. 4(a), x-direction fluctuation occurs and the wave vector of the magnetic pattern is directed in the x direction as shown in Fig. 4(b). The MDDI energy for this configuration is higher than that of Fig. 4(c), where y-direction fluctuation is induced. In other words, the MDDI energy is reduced by the magnetic fluctuation, and the reduction is larger in pattern (c) than in pattern (b). The reduction in MDDI energy is converted into kinetic energy ($\sim k^2$), which is higher at point Q than at point P in Fig. 4(a). This explains why the magnetic fluctuations change from x-direction to y-direction along the k_x axis.

Now, we investigate the magnetic fluctuations for the situation discussed in Sec. III B. The fluctuations are considered to be longitudinal or transverse. The longitudinal and transverse fluctuations are represented by $\delta\hat{f}_z$ and $\delta(\hat{f}_x + i\hat{f}_y)$, respectively. Substituting $\varphi = \varphi_0(1 + \delta\varphi)$ and $|\varphi_0|^2 = 1$ into Eq. (33), we obtain the expressions for the two types of fluctuations described by the first order of $\delta\varphi$ as $\delta\hat{f}_z = -\text{Re}(\delta\varphi)$ and $\delta(\hat{f}_x + i\hat{f}_y) = \varphi_0\text{Im}(\delta\varphi)$. Namely, the longitudinal and transverse fluctuations are characterized by the real and imaginary parts of $\delta\varphi$, respectively.

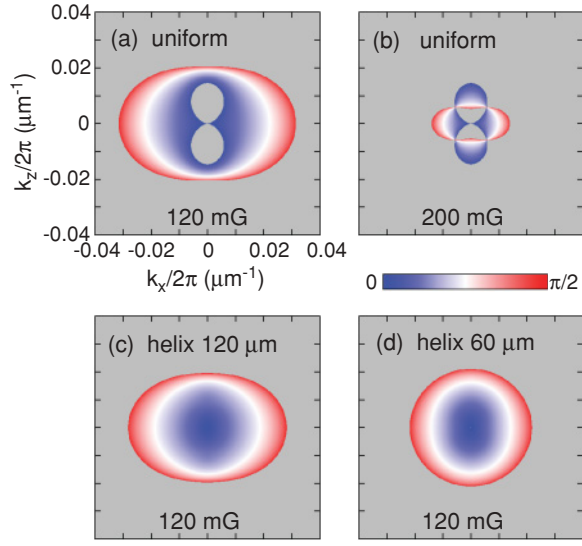We can also apply the above method to discuss the magnetic fluctuation preference, which is characterized by

FIG. 4. (Color) (a) Magnetic fluctuation preference $\theta(k)$ for the unstable mode shown in Fig. 2. The x-direction fluctuation is dominant in the red regions ($\pi/4 < \theta < \pi/2$) and the y-direction fluctuation is dominant in the blue regions ($0 < \theta < \pi/4$). (b) and (c) Schematic pictures of the magnetic patterns induced by the dynamical instability at points (b) P and (c) Q designated in (a). The arrows show the local magnetizations projected onto the x-y plane. The MDDI energy for configuration (c) is lower than that for (b).

FIG. 5. (Color) Magnetic fluctuation preference $\theta(\boldsymbol{k})$ for uniform and helical spin structures in the z direction with a pitch $2\pi/\kappa_\alpha$ μm under a strong magnetic field. The initial structure is uniform for (a) and (b), a helix with a pitch (c) 120 μm, and (d) 60 μm. The external field B is [(a), (c), and (d)] 120 mG and (b) 200 mG. The fluctuations are longitudinal in the red regions ($\pi/4 < \theta < \pi/2$) and transverse in the blue regions ($0 < \theta < \pi/4$). The other parameters are the same as those in Fig. 3.

$\theta = \tan^{-1}(A_{\mathrm{R}}/A_{\mathrm{I}})$, in the present case. Since $g_2 = g_2^*$, we can simplify Eq. (56) as

$$\theta(\boldsymbol{k}) = \tan^{-1}\sqrt{\frac{g_2 - g_1}{g_2 + g_1}}, \qquad (57)$$

where g_1 and g_2 are defined by Eqs. (49) and (50), respectively. The magnetic fluctuation is longitudinal if $\pi/4 < \theta < \pi/2$ and transverse if $0 < \theta < \pi/4$.

The wave-vector dependence of $\theta(\boldsymbol{k})$ for the unstable modes shown in Figs. 3(a), 3(c), 3(d), and 3(f) are demonstrated in Fig. 5. When the dynamical instability has a round shape [Figs. 5(a), 5(c), and 5(d)], the fluctuations are transverse for small k and longitudinal for large k. Figure 5(b) looks more complex than the schematics for the other cases: fluctuations are transverse for $\boldsymbol{k} \parallel \hat{z}$ and longitudinal for

$\boldsymbol{k} \parallel \hat{x}$. The magnetic fluctuation preference is consistent with that obtained by the Bogoliubov analysis [15,25], and discrepancies appear in strong fields for the same reason as that for the dynamical instability.

V. CONCLUSIONS

Employing our hydrodynamic description derived in Sec. II, we have demonstrated some simple examples of the analysis of dynamical instability and magnetic fluctuation preference in Secs. III and IV, respectively. Once one finds a stationary solution of the hydrodynamic equations, it is a straightforward task to obtain the analytical form of the dynamical instability: the only necessary step is the diagonalization of a 2×2 matrix. The eigenvalues and eigenvectors of the matrix lead to the dynamical instability and the magnetic fluctuation preference, respectively. Although we have discussed just a few types of spin structures and external fields for simplicity, our method can be applied to other conformations.

In conclusion, we have introduced the hydrodynamic equations for a ferromagnetic spinor dipolar BEC with an arbitrary spin by means of stereographic projection. This simple description provides a straightforward approach by which to investigate spin dynamics, i.e., dynamical instability and magnetization fluctuation preference, which are expressed in analytical forms. The description should also be useful for the study of the exact solutions of hydrodynamic equations of a spinor BEC.

APPENDIX: CONTRIBUTIONS FROM THE SHORT-RANGE INTERACTION, MDDI, AND LINEAR AND QUADRATIC ZEEMAN EFFECTS

The contribution from the short-range interaction to the equation of motion of f_z is calculated as

$$\left[\frac{\partial f_z}{\partial t}\right]_{\mathrm{s}} = \frac{1}{i\hbar}(F_z)_{mn}\left[\left(i\hbar\frac{\partial \Psi_m^*}{\partial t}\right)\Psi_n + \Psi_m^*\left(i\hbar\frac{\partial \Psi_n}{\partial t}\right)\right]_{\mathrm{s}}$$

$$= \sum_{S=0,\mathrm{even}}^{2F}\frac{4\pi\hbar}{iM}a_S\sum_{M_S=-S}^{S}\sum_{lm'l'}(F_z)_{mn}[-\langle ml|SM_S\rangle\langle SM_S|m'l'\rangle\Psi_l\Psi_{m'}^*\Psi_{l'}^*\Psi_n + \Psi_m^*\langle nl|SM_S\rangle\langle SM_S|m'l'\rangle\Psi_l^*\Psi_{m'}\Psi_{l'}]$$

$$= \sum_{S=0,\mathrm{even}}^{2F}\frac{4\pi\hbar}{iM}a_S\sum_{M_S=-S}^{S}\sum_{lm'l'}m\langle ml|SM_S\rangle\langle SM_S|m'l'\rangle[-\Psi_m\Psi_l\Psi_{m'}^*\Psi_{l'}^* + \Psi_m^*\Psi_l^*\Psi_{m'}\Psi_{l'}]$$

$$= \sum_{S=0,\mathrm{even}}^{2F}\frac{4\pi\hbar}{iM}a_S\sum_{M_S=-S}^{S}\sum_{mm'}(m-m')\langle m,M_S-m|SM_S\rangle\langle SM_S|m',M_S-m'\rangle\Psi_m^*\Psi_{M_S-m}^*\Psi_{m'}\Psi_{M_S-m'}$$

$$= \sum_{S=0,\mathrm{even}}^{2F}\frac{2\pi\hbar}{iM}a_S\sum_{M_S=-S}^{S}\left[\sum_{mm'}(m-m')\langle m,M_S-m|SM_S\rangle\langle SM_S|m',M_S-m'\rangle\Psi_m^*\Psi_{M_S-m}^*\Psi_{m'}\Psi_{M_S-m'}\right.$$

$$+ \sum_{ll'}(-l+l')\langle M_S-l,l|SM_S\rangle\langle SM_S|M_S-l',l'\rangle\Psi^*_{M_S-l}\Psi^*_l\Psi_{M_S-l'}\Psi_{l'}\Bigg]$$
$$= 0, \tag{A1}$$

where we have used $(F_z)_{mn} = m\delta_{mn}$. Here, $[\cdots]_s$ denotes that only those terms that come from the short-range interaction are extracted. In the following, this notation is applied to the contributions from the MDDI ($[\cdots]_{dd}$), linear ($[\cdots]_p$), and quadratic ($[\cdots]_q$) Zeeman effects. Since the short-range interaction (2) is invariant under spin rotation, $[\partial f_x/\partial t]_s$ and $[\partial f_y/\partial t]_s$ also vanish, which are shown in a similar way by choosing the spin quantization axis along the x and y directions, respectively.

The contribution from the MDDI to the equation of motion of spin is calculated as

$$\left[\frac{\partial f_\mu}{\partial t}\right]_{dd} = \frac{1}{i\hbar}(F_\mu)_{mn}\left[\left(i\hbar\frac{\partial\Psi^*_m}{\partial t}\right)\Psi_n + \Psi^*_m\left(i\hbar\frac{\partial\Psi_n}{\partial t}\right)\right]_{dd}$$
$$= \frac{c_{dd}}{i\hbar}(F_\mu)_{mn}\left[-b^*_\nu(F^*_\nu)_{ml}\Psi^*_l\Psi_n + \Psi^*_m b_\nu(F_\nu)_{nl}\Psi_l\right]$$
$$= \frac{c_{dd}}{i\hbar}b_\nu\Psi^*_m(F_\mu F_\nu - F_\nu F_\mu)_{mn}\Psi_n$$
$$= \frac{c_{dd}}{i\hbar}b_\nu i\epsilon_{\mu\nu\lambda}f_\lambda$$
$$= \frac{c_{dd}}{\hbar}(\boldsymbol{b}\times\boldsymbol{f})_\mu. \tag{A2}$$

We have used the relations $F^\dagger_\mu = F_\mu$ and $[F_\mu, F_\nu] = i\epsilon_{\mu\nu\lambda}F_\lambda$.

Suppose the magnetic field is applied parallel to the z axis. Then, the contribution from the linear Zeeman effect is calculated as

$$\left[\frac{\partial f_\mu}{\partial t}\right]_p = \frac{1}{i\hbar}(F_\mu)_{mn}\left[\left(i\hbar\frac{\partial\Psi^*_m}{\partial t}\right)\Psi_n + \Psi^*_m\left(i\hbar\frac{\partial\Psi_n}{\partial t}\right)\right]_p$$
$$= \frac{p}{i\hbar}(F_\mu)_{mn}\left[-(F^*_z)_{ml}\Psi^*_l\Psi_n + \Psi^*_m(F_z)_{nl}\Psi_l\right]$$
$$= \frac{p}{i\hbar}i\epsilon_{\mu z\nu}f_\nu$$
$$= \frac{p}{\hbar}(\hat{z}\times\boldsymbol{f})_\mu. \tag{A3}$$

The contribution from the quadratic Zeeman effect is calculated in the same way as that shown above.

$$\left[\frac{\partial f_\mu}{\partial t}\right]_q = \frac{1}{i\hbar}(F_\mu)_{mn}\left[\left(i\hbar\frac{\partial\Psi^*_m}{\partial t}\right)\Psi_n + \Psi^*_m\left(i\hbar\frac{\partial\Psi_n}{\partial t}\right)\right]_q$$
$$= \frac{q}{i\hbar}(F_\mu)_{mn}\left[-(F^{*2}_z)_{ml}\Psi^*_l\Psi_n + \Psi^*_m(F_z)^2_{nl}\Psi_l\right]$$
$$= \frac{q}{i\hbar}\Psi^*_m(F_z[F_\mu, F_z] + [F_\mu, F_z]F_z)_{mn}\Psi_n$$
$$= \frac{q}{i\hbar}i\epsilon_{\mu z\nu}\Psi^*_m(F_\nu F_z + F_z F_\nu)_{mn}\Psi_n$$
$$= \frac{2q}{\hbar}n_{tot}\epsilon_{\mu z\nu}\hat{\mathcal{N}}_{z\nu}, \tag{A4}$$

where $\hat{\mathcal{N}}_{\mu\nu}$ is a nematic tensor defined by

$$\hat{\mathcal{N}}_{\mu\nu} = \tfrac{1}{2}\zeta^*_m(F_\mu F_\nu + F_\nu F_\mu)_{mn}\zeta_n. \tag{A5}$$

[1] T.-L. Ho and V. B. Shenoy, Phys. Rev. Lett. **77**, 2595 (1996).
[2] M. Nakahara, T. Isoshima, K. Machida, S. Ogawa, and T. Ohmi, Physica B **284-288**, 17 (2000); T. Isoshima, M. Nakahara, T. Ohmi, and K. Machida, Phys. Rev. A **61**, 063610 (2000).
[3] A. E. Leanhardt, Y. Shin, D. Kielpinski, D. E. Pritchard, and W. Ketterle, Phys. Rev. Lett. **90**, 140403 (2003).
[4] H. Mäkelä, Y. Zhang, and K.-A. Suominen, J. Phys. A **36**, 8555 (2003); H. Mäkelä, *ibid.* **39**, 7423 (2006).
[5] F. Zhou, Phys. Rev. Lett. **87**, 080401 (2001).
[6] G. W. Semenoff and F. Zhou, Phys. Rev. Lett. **98**, 100401 (2007).
[7] M. Kobayashi, Y. Kawaguchi, M. Nitta, and M. Ueda, Phys. Rev. Lett. **103**, 115301 (2009).
[8] L. E. Sadler, J. M. Higbie, S. R. Leslie, M. Vengalattore, and D. M. Stamper-Kurn, Nature (London) **443**, 312 (2006).
[9] M. Vengalattore, S. R. Leslie, J. Guzman, and D. M. Stamper-Kurn, Phys. Rev. Lett. **100**, 170403 (2008).
[10] M. Vengalattore, J. Guzman, S. R. Leslie, F. Serwane, and D. M. Stamper-Kurn, Phys. Rev. A **81**, 053612 (2010).
[11] For review of dipolar BECs, see T. Lahaye, C. Menotti, L. Santos, M. Lewenstein, and T. Pfau, Rep. Prog. Phys. **72**, 126401 (2009).
[12] L. Santos and T. Pfau, Phys. Rev. Lett. **96**, 190404 (2006).
[13] Y. Kawaguchi, H. Saito, and M. Ueda, Phys. Rev. Lett. **96**, 080405 (2006); **97**, 130404 (2006).
[14] S. Yi and H. Pu, Phys. Rev. Lett. **97**, 020401 (2006).
[15] Y. Kawaguchi, H. Saito, K. Kudo, and M. Ueda, Phys. Rev. A **82**, 043627 (2010).
[16] M. Takahashi, S. Ghosh, T. Mizushima, and K. Machida, Phys. Rev. Lett. **98**, 260403 (2007); J. A. M. Huhtamäki, M. Takahashi, T. P. Simula, T. Mizushima, and K. Machida, Phys. Rev. A **81**, 063623 (2010).
[17] A. Lamacraft, Phys. Rev. A **77**, 063622 (2008).
[18] R. Barnett, D. Podolsky, and G. Refael, Phys. Rev. B **80**, 024420 (2009).
[19] A. Lamacraft, Phys. Rev. B **81**, 184526 (2010).
[20] T.-L. Ho, Phys. Rev. Lett. **81**, 742 (1998).
[21] N. D. Mermin and T.-L. Ho, Phys. Rev. Lett. **36**, 594 (1976).
[22] S. Zhang and Z. Li, Phys. Rev. Lett. **93**, 127204 (2004); A. Thiaville, Y. Nakatani, J. Miltat, and Y. Suzuki, Europhys. Lett. **69**, 990 (2005).
[23] Y. Kawaguchi, H. Saito, and M. Ueda, Phys. Rev. Lett. **98**, 110406 (2007).
[24] M. Lakshmanan and K. Nakamura, Phys. Rev. Lett. **53**, 2497 (1984).
[25] R. W. Cherng and E. Demler, Phys. Rev. Lett. **103**, 185301 (2009).